Rapid Substrate Translocation by the Multisubunit, Erythroid Glucose Transporter Requires Subunit Associations but Not Cooperative Ligand Binding†

Peter E. Coderre, Erin K. Cloherty, Ralph J. Zottola, and Anthony Carruthers*

Program in Molecular Medicine, Department of Biochemistry and Molecular Biology, University of Massachusetts Medical School, Two Biotech, 373 Plantation Street, Worcester, Massachusetts 01605

Received February 15, 1995; Revised Manuscript Received April 19, 1995⊗

ABSTRACT: The human erythroid glucose transporter is a GLUT1 homotetramer whose structure and function are stabilized by noncovalent, cooperative subunit interactions. The present study demonstrates that exofacial tryptic digestion of GLUT1 abolishes cooperative interactions between substrate binding sites on adjacent subunits under circumstances where subunit associations and high catalytic turnover are maintained. Extracellular trypsin produces rapid, quantitative cleavage of the human red cell-resident sugar transport protein, GLUT1. One major carboxyl-terminal peptide of $M_{r(app)}$ 25 000 is detected by immunoblot analysis. Endofacial tryptic digestion of GLUT1 results in the complete loss of GLUT1 carboxyl-terminal structure. GLUT1-mediated erythrocyte sugar uptake, transport inhibition by cytochalasin B, and GLUT1 oligomeric structure are unaffected by exofacial GLUT1 proteolysis. In contrast, the cytochalasin B binding capacity of GLUT1 and the $K_{d(app)}$ for cytochalasin B binding to the transporter are doubled following exofacial tryptic digestion of GLUT1. Photoaffinity labeling experiments show that increased cytochalasin B binding results from increased ligand binding to the 25 kDa carboxyl-terminal GLUT1 peptide. Proteolysis abolishes allosteric interactions between sugar import (maltose binding) and sugar export (cytochalasin B binding) sites that normally exist on adjacent subunits within the transporter complex, but interact with negative cooperativity. Following exofacial proteolysis, these sites become mutually exclusive. Dithiothreitol disrupts GLUT1 quaternary structure, inhibits 3-*O*-methylglucose transport, and abolishes cooperative interactions between sugar import and export sites in control cells. Studies with reconstituted purified GLUT1 confirm that the action of trypsin on cytochalasin B binding is direct, show that proteolysis increases the apparent affinity of the sugar efflux site for transported sugars, and suggest that the membrane bilayer stabilizes GLUT1 noncovalent structure and catalytic function following GLUT1 proteolysis. Collectively, these findings demonstrate that GLUT1 does not require an intact polypeptide backbone for catalytic function. They show that the multisite sugar transporter mechanism is converted to a simple ping-pong carrier mechanism following exofacial GLUT1 proteolysis. They reveal that subunit cooperativity can be lost under circumstances where cohesive structural interactions between transporter subunits are maintained. They also refute the hypothesis [Hebert, D. N., & Carruthers, A. (1992) *J. Biol. Chem. 267*, 23829−23838] that rapid substrate translocation by the multisubunit erythroid glucose transporter requires cooperative interactions between subunit ligand binding sites.

Sugars penetrate cells by three mechanisms (Stein, 1986): slow transbilayer diffusion; rapid protein-mediated, facilitated diffusion (uniport;) and rapid, protein-mediated cotransport (symport). Glucose uniport is found in all mammalian cells (Stein, 1986), is characteristic of a large number of E1·E2 uniport and antiport transport systems (Stein, 1986), and provides the cell with sugars for ATP synthesis, maintenance of cellular redox potential, and covalent modification and processing of glycoproteins and glycolipids. Impaired *cellular* glucose uniport disturbs organismal carbohydrate homeostasis (Mueckler, 1993). Impaired *intracellular* glucose transport is found in some forms of glycogen storage disease (Waddell et al., 1992; Waddell & Burchell, 1993), and impaired *transcellular* glucose transport leads to developmental delay and seizures when expressed at the blood/brain barrier, the choroid plexus, and in glia and neurons of the brain (De Vivo et al., 1991; Harik, 1992). These considerations indicate that normal glucose uniport function is vital for both cellular and organismal homeostasis. In spite of its biological importance, the molecular mechanism of glucose uniport is not understood (Naftalin & Holman, 1977; Stein, 1986; Carruthers, 1990; Gould & Holman, 1993).

GLUT1[1] is the most abundant sugar transport protein in mammals. This transport protein is found in almost all tissues, but is especially abundant in the erythrocytes of primates (Sogin & Hinkle, 1980) and at blood/tissue barriers [e.g., capillary endothelia of the brain (Maher et al., 1993),

† This work was supported by NIH Grants DK 44888 and DK 36081.
* Author to whom correspondence should be addressed.
⊗ Abstract published in *Advance ACS Abstracts,* July 1, 1995.

[1] Abbreviations: GLUT1, erythrocyte glucose transporter; 3OMG, 3-*O*-methylglucose; C-IgG, anti-GLUT1 carboxyl-terminal peptide antiserum; ∂-Ab, antitetrameric GLUT1 rabbit antiserum; CCB, cytochalasin B; DTT, dithiothreitol; EDTA, ethylenediaminetetraacetic acid; FBS, fetal bovine serum; HEPES, (*N*-(2-hydroxyethyl)piperazine-*N*′-[2-ethanesulfonic acid]); PAGE, polyacrylamide gel electrophoresis; SDS, sodium dodecyl sulfate; Tris-HCl, tris(hydroxymethyl)aminomethane hydrochloride; V8, Endoproteinase glu-C; V9, endoproteinase lys-C; PMSF, phenylmethanesulfonyl fluoride.

0006-2960/95/0434-9762$09.00/0 © 1995 American Chemical Society

retina (Takata et al., 1992a), and the syncytiotrophoblast and capillary endothelia of the placenta (Takata et al., 1992b)]. This is particularly important in the brain where glucose is the major fuel for metabolism. GLUT1 has been purified from human erythrocytes where, as in CHO cells, rat and 3T3-L1 adipocytes, and nucleated erythrocytes, it exists as a homotetramer (Jung et al., 1980; Hebert & Carruthers, 1992; A. Carruthers, A. L. Helgerson, unpublished observations; Harrison et al., 1991; Diamond & Carruthers, 1993). GLUT1 does not form heterocomplexes with other naturally occurring sugar transporter isoforms within the same cell (Pessino et al., 1991).

The kinetic mechanism of GLUT1-mediated sugar transport is not a simple ping-pong mechanism as originally proposed (Widdas, 1952). Rather, the transporter binds sugars simultaneously at import and export sites (Carruthers, 1986a,b, 1991; Chin et al., 1992; Hebert & Carruthers, 1992; Helgerson & Carruthers, 1987, 1989; Janoshazi & Solomon, 1993; Naftalin, 1988; Naftalin & Rist, 1994). Each subunit (GLUT1 protein) of the transporter (tetrameric GLUT1) is catalytically active and contributes a single substrate binding site (import or export) at any instant (Hebert & Carruthers, 1992). However, subunit interactions are thought to give rise to a pseudo-D2 substrate binding site arrangement where, at any instant, two subunits must present import sites and two subunits present export sites (Hebert & Carruthers, 1992). This is hypothesized to accelerate transport because sugar uptake by one subunit is coupled to the simultaneous regeneration of import sites on adjacent subunits (Hebert & Carruthers, 1992). This theory is supported by the demonstration that the catalytic turnover of dimeric GLUT1 [which lacks subunit cooperativity (Hebert & Carruthers, 1992)] is considerably lower than that of parental tetrameric GLUT1 (Appleman & Lienhard, 1989; Lowe & Walmsley, 1986). In the present study, we provide new information about subunit interactions in the transporter complex and refute the hypothesis that cooperative interactions between subunit ligand binding sites are required for high catalytic turnover of GLUT1.

In the course of our studies, we have observed that human red cell-resident GLUT1 is proteolytically cleaved by extracellular trypsin. Initially, this result was unexpected since trypsin is known to inhibit GLUT1-mediated sugar transport only when present inside the red cell (Baldwin et al., 1980; Carruthers & Melchior, 1983; Masaik & LeFevre, 1977), where it acts to proteolytically cleave GLUT1 (Cairns et al., 1987; Holman & Rees, 1987; Mueckler et al., 1985). While the effect of exofacial trypsin on GLUT1 covalent structure is unreported, immunoblot analyses show that the rat adipocyte glucose transport protein GLUT4 is digested by exofacial trypsin (Czech & Buxton, 1993). GLUT1 and GLUT4 share 67% sequence identity and similar (proposed) membrane topographies in which both transporters are suggested to expose extracellular tryptic cleavage sites (Fukumoto et al., 1989). It is not surprising, therefore, that GLUT1 is also cleaved by exofacial trypsin. The functional resistance of GLUT1 to exofacial trypsin indicates, therefore, that GLUT1-mediated sugar transport is unaffected by exofacial GLUT1 proteolysis.

Closer examination reveals that exofacial GLUT1 proteolysis uncouples cooperative interactions between substrate binding sites on adjacent subunits without causing subunit dissociation or inhibition of sugar transport. Extracellular reductant, however, causes tetrameric GLUT1 dissociation, transport inhibition, and loss of cooperative ligand binding to GLUT1. This suggests that the higher catalytic turnover of tetrameric GLUT1 does not derive from functional cooperativity between ligand binding sites as originally proposed (Hebert & Carruthers, 1992), but rather from other aspects of subunit interactions within the tetrameric transporter complex.

MATERIALS AND METHODS

Materials. Endoproteinase glu-C (V8), endoproteinase lys-C (V9), and sequence-grade trypsin were obtained from Boehringer-Mannheim Indianapolis, IN). Sugars, cytochalasins, phloretin, thrombin, TPCK-treated trypsin (type XIII), and soybean trypsin inhibitor were obtained from Sigma Chemical Co. (St. Louis, MO). [^{3}H]Cytochalasin B, [^{125}I]-protein A, and [^{3}H]-3-*O*-methylglucose (3OMG) were purchased from New England Nuclear (DuPont) (Wilmington, DE). Rabbit antisera raised against a synthetic carboxyl-terminal peptide of GLUT1 (intracellular residues 480−492; C-Ab) were obtained from East Acres Biologicals (Southbridge, MA). Anti-GLUT1 antisera reacting with extracellular epitopes of GLUT1 (∂-Ab) were prepared as described previously (Harrison et al., 1990). Fluorescein-conjugated goat anti-rabbit IgG antiserum was obtained from Calbiochem (La Jolla, CA). Fetal bovine serum was purchased from Upstate Biotechnology Inc. (Lake Placid, NY).

Solutions. Saline consisted of 150 mM NaCl, 2 mM EDTA, and 5 mM HEPES (pH 7.4). Lysis medium consisted of 5 mM HEPES and 0.2 mM EDTA (pH 8). Tris medium consisted of 50 mM Tris-HCl (pH 7.4). Cytochalasin stock solutions were made in dimethyl sulfoxide. Phloretin stock solutions were made in ethanol. Carrier concentrations in cytochalasin- and phloretin-containing solutions were never greater than 0.1%. Stop solution contained 150 mM NaCl, 5 mM Tris-HCl, 20 μM cytochalasin B, 100 μM phloretin, 2 μM $HgCl_2$, and 1 mM KI (pH 7.4, 0−2 °C).

Preparation of Red Cells and Ghosts. Human red cells were collected from recently expired, whole human blood (University of Massachusetts Medical Center Blood Bank) by suspension in ice-cold saline (25 vol of saline:1 vol of whole blood), followed by centrifugation at 1100*g* for 5 min. The supernatant fluid and buffy coat were aspirated, and the red cell pellet was resuspended in saline. This wash/centrifugation procedure was repeated until the supernatant fluid was clear and the red cell pellet lacked any discernible buffy coat (normally 3−4 cycles). The washed red cells were then resuspended in 100 vol of saline and allowed to rest at room temperature for 1 h to deplete intracellular D-glucose. D-Glucose-depleted cells were harvested by centrifugation to a final hematocrit of 80−90%.

Red cell ghosts were prepared from washed, intact red cells as in Helgerson et al. (1989), using saline and lysis medium described earlier. Red cell ghosts were depleted of peripheral membrane proteins by a single high-pH wash as in Carruthers (1986a).

Purification and Reconstitution of GLUT1. GLUT1 was purified from human erythrocyte membranes in the absence of reductant (Hebert & Carruthers, 1992) and was reconstituted into egg phosphatidylcholine large unilamellar vesicles (diameter $\approx$ 2 μm, as judged by phase contrast microscopy) by cholate dialysis (Hebert & Carruthers, 1991; Zeidel et

al., 1992). Equilibrium ligand (sugar or cytochalasin B) binding to reconstituted GLUT1 proteoliposomes was measured by monitoring ligand-induced quenching of GLUT1 intrinsic tryptophan fluorescence (Hebert & Carruthers, 1992). GLUT1-mediated D-glucose uptake by reconstituted proteoliposomes was measured by light-scattering analysis of sugar transport-induced changes in proteoliposomal volume (Carruthers & Melchior, 1983, 1984a,b). The orientation of GLUT1 in reconstituted, sealed proteoliposomes was determined by the use of antibodies that react with endofacial (C-Ab) or exofacial (∂-Ab) epitopes of erythrocyte GLUT1, as described previously (Zeidel et al., 1992). Our results (63% right side out:37% inside out) are consistent with previous demonstrations of random GLUT1 orientation upon reconstitution (Baldwin et al., 1980; Carruthers & Melchior, 1984a; Zeidel et al., 1992).

Proteolysis of GLUT1. Packed red cells (0.5 mL) were suspended in saline to a final volume of 1.5 mL. Samples were warmed to 37 °C for 10 min, and to this mixture was added either saline or trypsin (final concentration ≤ 1 mg/mL). Cell slurries were mixed by end-over-end rotation and incubated at 37 °C for 30 min. Reactions were terminated by the addition of 12 mL of saline containing 0.2 mM PMSF. Cells were collected by centrifugation, resuspended in PMSF−saline, and then stored on ice until use.

Immunoblot Analysis of GLUT1. Membranes were collected by centrifugation and resuspended in 50 mM Tris-HCl (pH 7.4). Proteins were resolved on either 10% or 15% gels as described previously (Laemmli, 1970), transferred to Immobilon P membrane filters, and subjected to Western analysis using C-Ab and [^{125}I]protein A as reporter molecules. Filters were dried and exposed to Kodak XAR-5 film at −70 °C for 2−48 h using a DuPont Cronex Lightning Plus intensifying screen. The resulting autoradiograms were quantitated by densitometry using a Hoefer GS300 transmittance/reflectance scanning densitometer in combination with the GS-370 data system (Apple Macintosh Version). Peaks were integrated and expressed as a percentage of total transmittance.

Photolabeling GLUT1 Using [^{3}H]Cytochalasin B. Red cells were preincubated in saline containing [^{3}H]cytochalasin B (3.7 μM, 50 μCi) plus 10 μM cytochalasin D ± D- or L-glucose (200 mM) for 20 min on ice. The suspension was irradiated at 300 nm for 0.5 min in a Rayonett photoreactor. Cells were collected by centrifugation and washed by resuspension in 10 vol of saline. The centrifugation/wash cycle was repeated twice.

Cytochalasin B Binding to Erythrocyte Membranes. Equilibrium [^{3}H]cytochalasin B binding measurements were as described by Helgerson and Carruthers (1987). The cytocrit of the final suspension of ghosts in [^{3}H]cytochalasin B solution was 33%. Initial studies of maltose inhibition of cytochalasin B binding to intact cells used Sigma plant biology-grade sucrose as the osmotic substitute or control for extracellular maltose. This source, however, was discovered to be significantly contaminated with D-glucose, a GLUT1 substrate that acts as a competitive inhibitor of exofacial maltose binding to GLUT1 and, following its transport into the cell, as a competitive inhibitor of cytochalasin B binding to GLUT1. Subsequent experiments used Sigma ACS-grade sucrose. In experiments where cytochalasin B binding was measured in the presence of DTT, solutions were made daily.

3-O-Methylglucose Transport by Erythrocytes. Zero trans uptake and efflux of a nonmetabolized but transported sugar (3-*O*-methylglucose) by red cells at ice temperature were measured using [^{3}H]-3OMG as described previously (Helgerson & Carruthers, 1989; Helgerson et al., 1989). Sugar-free red cells (at ice temperature) were exposed to 5 vol of saline (ice temperature) containing variable [3OMG]. Uptake was permitted to proceed, and then 50 vol (relative to cell volume) of stop solution was added to the cell suspension. Cells were sedimented, washed twice in stop solution, collected by centrifugation, and extracted in 1 mL of 3% perchloric acid. Non-protein-mediated 3OMG uptake (leakage) was measured in parallel in each experiment by preincubating cells with 50 μM cytochalasin B (a transport inhibitor, $K_{i(app)}$, for noncompetitive inhibition of uptake is 375 nM; see Table 1). Cytochalasin B (50 μM) was also included in the uptake medium during these uptake measurements. In the studies reported here, 3OMG uptake by cells and ghosts was 90% inhibited by 50 μM cytochalasin B.

Our measurements show that 3OMG uptake by intact cells is characterized by a maximum, pseudo-first-order rate constant (V_{max}/K_m) of 0.2 min^{-1} or a half-time for uptake at limitingly low [3OMG] of 208 s. In the studies described here, we employed 10 or 30 s intervals for uptake determinations in order to limit the 3OMG space of the cells to 10% or lower. Equilibrium 3OMG spaces were determined from 1 h incubations at 37 °C. The use of this 10 or 30 s sampling period results in the overestimation of $K_{m(app)}$ for sugar uptake by less than 7% without affecting the reliability of estimates of V_{max} (Helgerson et al., 1989).

Calculation of Transport and Ligand Binding Parameters. V_{max} and $K_{m(app)}$ for 3OMG uptake were computed by direct, nonlinear regression analysis of the concentration dependence of 3OMG uptake, assuming Michaelis−Menten kinetics. $K_{d(app)}$ and B_{max} for ligand (cytochalasin B and D-glucose) binding to GLUT1 were computed in a similar manner. Here, however, we modeled the data by assuming two saturable components of ligand binding. When the computed $K_{d(app)}$ for binding to the first saturable component was statistically indistinguishable from $K_{d(app)}$ for binding to the second saturable component, we concluded that binding was described by a single saturable process. Otherwise, we concluded that the assumption of multicomponent saturable binding is correct. In these instances, the addition of a third or fourth saturable component to the analysis did not statistically improve the computed fit. The software package used was KaleidaGraph 3.0 (Synergy Software, Reading, PA).

Quantitation of Antibody Binding to Red Cell GLUT1. Two methods were used: immunofluorescence microscopy (see the following) and direct binding measurements using [^{125}I]protein A as the reporter molecule (Harrison et al., 1990; Diamond & Carruthers, 1993). ∂-Ab IgG's were also affinity-purified by using 500 μg of purified GLUT1 that was additionally gel-purified by reducing SDS−PAGE and subsequently transferred to Immobilon. That region of the blot containing intact GLUT1 ($M_{r(app)}$ = 45000−68000) was excised, blocked using 3% gelatin, and then incubated with ∂-Ab for 2 h at room temperature as per Western blotting protocols (Harrison et al., 1990; Diamond & Carruthers, 1993). The membrane was washed, and IgG's were eluted using 100 mM glycine (pH 2.5, 10 min of incubation). The buffer was removed, neutralized using 0.1 vol of 1 M Tris

Table 1: Effect of Extracellular Trypsin on Ligand Binding to Red Cell GLUT1

		control[a]	trypsin
CCB binding to			
intact cells[b]	$K_{d(app)}$ (nM)	102 ± 40	324* ± 66
	B_{max} (sites/cell)[c]	262000 ± 23000	508700* ± 48000
membranes from intact cells[d]			
	$K_{d(app)}$ (nM)	86 ± 17	155* ± 31
	B_{max} (sites/cell)	169200 ± 14400	271440* ± 32572
membranes from leaky cells[e]			
	$K_{d(app)}$ (nM)	103 ± 32	not detected
	B_{max}	120240 ± 21960	not detected
proteoliposomes[f]	$K_{d(app)}$ (nM)	140 ± 15	353* ± 28
	B_{max} (% quench)[g]	6.4 ± 0.2	6.0 ± 0.2
D-glucose binding to proteoliposomes[h]			
	$K_{d(low)}$ (mM)	0.10 ± 0.04	0.07 ± 0.05
	$B_{max(low)}$ (% quench)[g]	1.37 ± 0.16	1.95 ± 0.64
	$K_{d(high)}$ (mM)	17.45 ± 3.52	3.8* ± 1.6
	$B_{max(high)}$ (% quench)[g]	5.25 ± 0.27	4.4 ± 0.6

[a] All experiments are paired experiments (control versus trypsin treatment). The number of paired determinations made in duplicate is three or greater. *Indicates that the result is significantly different from the control measurement ($p < 0.05$, 1 tailed t-test). [b] Cytochalasin B binding was measured in intact erythrocytes following either control or trypsin (100 μg of trypsin/1 × 10^9 cells; 30 min at 37 °C) treatment. [c] B_{max} for cytochalasin B binding in molecules of cytochalasin B bound per unit cell membrane (each cell membrane contains 0.6 pg of protein). [d] Cytochalasin B binding was measured in erythrocyte membranes isolated from either control or trypsin-treated erythrocytes (100 μg of trypsin/1 × 10^9 cells; 30 min at 37 °C). [e] Cytochalasin B binding was measured in erythrocyte membranes obtained following either control or trypsin treatment (100 μg of trypsin/1 × 10^9 cells; 30 min at 37 °C) of unsealed erythrocyte membranes. [f] Cytochalasin B binding was measured in reconstituted GLUT1 proteoliposomes following either control or trypsin treatment (5 μg of trypsin/20 μg of GLUT1). [g] Binding was measured by analysis of ligand-induced quenching of GLUT1 intrinsic fluorescence. Maximum binding is represented by maximum quench (% of original fluorescence) induced by the ligand. [h] D-glucose binding to GLUT1 is characterized by high- and low-affinity components. Binding was measured at 24 °C following control and trypsin (5 μg/20 μg of GLUT1; 30 min at 37 °C) treatments.

(pH 8.0), and dialyzed overnight against 100 vol of saline. This was used for subsequent binding studies using [^{125}I]-protein A or ELISA. Our measurements show that 87 ± 4% [208 721 ± 9276 versus 240 778 ± 1655 cpm] of the red cell binding activity in 5 μL of ∂-Ab serum is recovered following ∂-Ab purification using denatured, reduced, intact GLUT1 as the affinity matrix. ELISA indicates superimposable ∂-Ab and ∂-Ab−IgG titration curves when the concentration of recovered material is adjusted for dilution during purification.

For immunofluorescence microscopy, cells were first attached to polylysine-coated coverslips. Circular coverslips were washed in 70% ethanol and 1% HCl for 1 h, oven-dried, immersed in a 10% solution of polylysine for 5 min, then air-dried overnight. Washed erythrocytes were exposed to saline ± trypsin (0.5 mg mL^{-1}) for 30 min at 37 °C and then washed free of trypsin. These cells (10 μL, 50% Ht) were pipeted onto polylysine-coated coverslips positioned above 5 mL of saline in 50 mL Falcon tubes. These tubes were then centrifuged at 1100g for 5 min, and unattached cells were removed by addition and subsequent aspiration of saline (20 mL). Two additional saline washes were made, and then the erythrocyte-coated coverslips were transferred to six-well tissue culture dishes for immunohistochemical processing.

Coverslips with attached control and trypsin-treated cells were exposed to saline ± 2 mM dithiothreitol (pH 7.4) for 30 min at 37 °C. At this time, cells were fixed by the addition of 4% paraformaldehyde (15 min) and then washed twice in saline. Fixed cells were permeabilized by 15 min of incubation in saline containing 0.05% Triton X-100 and 1% fetal bovine serum (FBS), followed by four washes in saline containing 1% FBS. Cells were incubated for 60 min in saline containing 1% FBS and either C-Ab (1:5000 dilution) or ∂-Ab (1:5000 dilution), washed three times in FBS−saline, and then incubated for 30 min with fluorescein-conjugated goat-anti rabbit IgG's (1:250 dilution). Coverslips were washed three times in saline and mounted on a slide with 2.5% DABCO (Sigma Chemicals) and 90% glycerol, and the slides were sealed with clear Cover Girl™ nail polish.

Samples were visualized by fluorescence microscopy using a Nikon Diaphot 200 microscope with a Nikon Apo 60/1.4 oil immersion lens. Images were digitized with 24-bit resolution using a thermoelectrically cooled CCD camera (Photometrics Ltd., Tuscon, AZ) and stored on magnetic medium for subsequent analysis.

Nondenaturing Size-Exclusion Chromatography. Size-exclusion chromatography was carried out using a Toso Haas TSK-Gel G4000-SWXL column as described in Hebert and Carruthers (1981). The column was calibrated using Pharmacia standards. The calibration is log(Stokes radius in nm) = $1.551-1.801K_{av}$ ($R^2 = 0.9714$).

RESULTS

Effects of Trypsin on GLUT1 Covalent Structure. Intact erythrocytes were treated with several proteases, including thrombin, endoproteinase glu-C, endoproteinase lys-C, and trypsin. These proteases show high specificity for arginine, glutamic acid, lysine, and arginine/lysine residues, respectively. Only extracellular trypsin (Figure 1A, lane 1) cleaves erythrocyte-resident GLUT1. Identical results were obtained using three different batches of TPCK−trypsin and four batches of sequence-grade trypsin, and the effects of trypsin are blocked by soy bean trypsin inhibitor (10:1 inhibitor to trypsin ratio by mass; $n = 2$). Tryptic cleavage generates a 25 100 Da GLUT1 C-terminal fragment as judged by immunoblot analysis using GLUT1 C-terminal peptide antiserum (C-Ab). Since intact GLUT1 is also found under these conditions, the possibility exists that either some erythrocytes are leaky and thus allow endofacial tryptic

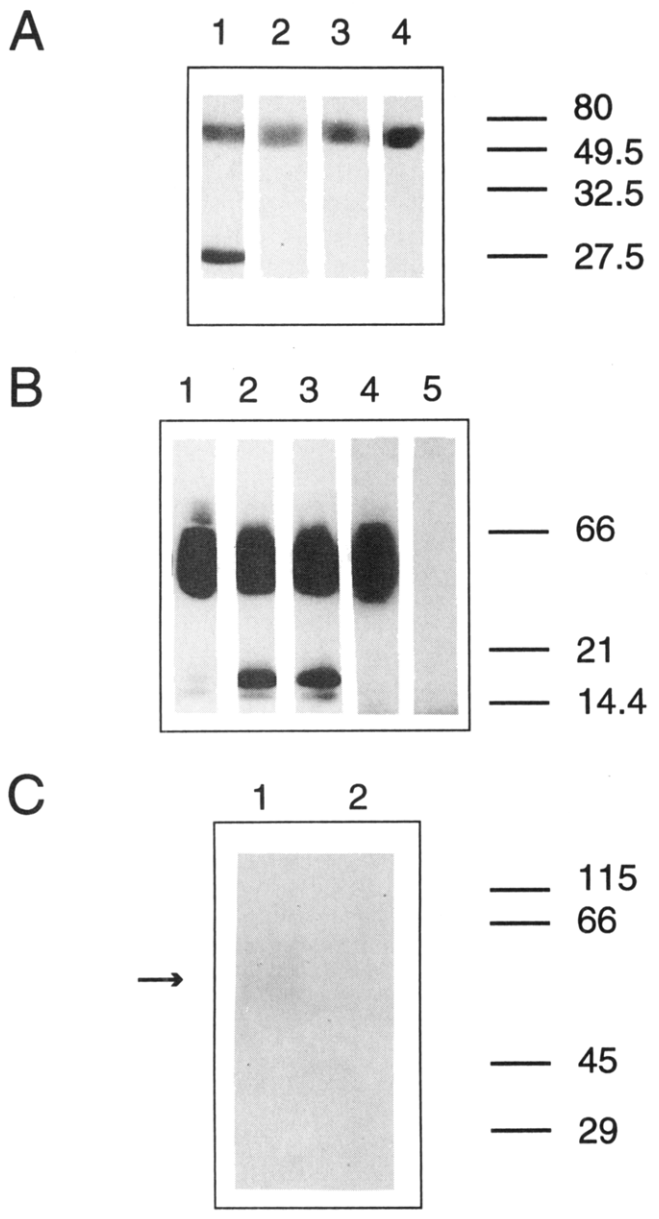

FIGURE 1: Tryptic digestion of erythrocyte GLUT1. (A) Western blot analysis of human erythrocyte membranes using anti-GLUT1 C-terminal antiserum. Intact erythrocytes (5×10^9 cells) in 1 mL of saline were exposed to 200 μg of trypsin (lane 1), thrombin (lane 2), V8 (lane 3), or V9 (lane 4) for 30 min at 37 °C. Cells were collected, washed, and lysed, and membrane proteins were resolved on 15% acrylamide gels. (B) Western blot analysis of human erythrocyte membranes using anti-GLUT1 C-terminal antiserum. Intact erythrocytes (1×10^{10} cells) were incubated in saline (lane 1), or in 2 mL of saline containing 100 μg of trypsin (lane 2), or in trypsin and 100 μM cytochalasin B (lane 3) at 37 °C for 1 h. Cell membrane proteins were resolved on 10% acrylamide gels. In lanes 4 and 5, unsealed erythrocyte ghosts (4 mg of membrane protein in 2 mL of saline) were incubated with (lane 5) or without (lane 4) 100 μg of trypsin for 15 min. (C) Coomassie-stained gel (10% acrylamide) of reconstituted GLUT1 proteoliposomes (20 μg of GLUT1 in 10 mg of egg phosphatidylcholine) exposed to 100 μL of saline (lane 1) or 100 μL of saline containing 5 μg of trypsin (lane 2) at 37 °C for 30 min. The mobility of prestained molecular weight markers is indicated in panels A−C.

cleavage of GLUT1 or that suboptimal conditions were used for exofacial tryptic digestion.

In contrast to its effects on GLUT1 in intact red cells, tryptic digestion of unsealed, erythrocyte membranes results in the complete loss of immunodetectable glucose transporter (Figure 1B, lane 5). Because peptide maps obtained from intact cells and unsealed ghosts differ significantly, these results strongly suggest that exofacial trypsin acts at an extracellular GLUT1 site in intact red cells. Maximum tryptic cleavage of erythrocyte-resident GLUT1 is obtained within 30−40 min of exposure to trypsin (Figure 2A,B). Cleavage appears to occur at at least two sites. At early times, a low-abundance 38 kDa C-terminal GLUT1 fragment is just detectable (≤8% total immunoreactive protein as judged by densitometric analysis). This fragment is lost upon longer exposure to trypsin. Maximal GLUT1 digestion is produced at a trypsin to membrane protein ratio of approximately 1:100 (3 μg of trypsin per 5×10^8 cells; Figure 2C). At higher trypsin concentrations, the dependence of the rate of proteolysis upon trypsin level becomes nonlinear. This may result from trypsin autodigestion. Exofacial tryptic digestion of red cell-resident GLUT1 is unaffected by the presence of 2 mM DTT (pH 7.4, $n = 3$).

Effects of Trypsin on GLUT1 Oligomeric Structure. We were curious to understand whether disruption of the GLUT1 backbone affects GLUT1 oligomeric structure. GLUT1 is known to exist as a GLUT1 homotetramer in the erythrocyte membrane (Hebert & Carruthers, 1991, 1992). We examined the effects of exofacial tryptic cleavage on GLUT1 oligomeric structure by monitoring the binding of ∂-Ab to intact red cells. ∂-Ab is an epitope-specific antiserum that binds with high affinity to tetrameric GLUT1, but fails to bind to dimeric GLUT1 (Hebert & Carruthers, 1992). ∂-Ab binding to intact cells (212 987 ± 2166 cpm per 2×10^8 cells; $n = 3$) is unaffected by prior erythrocyte exposure to exofacial trypsin (191 789 ± 2427 cpm per 2×10^8 cells; $n = 3$). This confirms that epitopes exposed in tetrameric GLUT1, but not in dimeric GLUT1, remain accessible in the trypsin-treated transporter and strongly suggests that transporter oligomeric structure is preserved under conditions where the polypeptide backbone of each subunit is broken. Quantitative immunofluorescence digital imaging fluorescence microscopy (Figure 3) confirms this result and further shows that exposure of red cells to 2 mM DTT for 30 min at 37 °C prior to fixation reduces ∂-AB binding to control and trypsin-treated red cells by 80% and 70%, respectively. C-Ab binding to permeabilized control and trypsinized cells is not inhibited by DTT.

We further examined the oligomeric structure of GLUT1 by using nondenaturing size-exclusion chromatography to determine the hydrodynamic radius of GLUT1-containing micelles solubilized from erythrocyte membranes. The Stokes radius of C-Ab-reactive, protein-containing cholic acid/lipid micelles solubilized from red cell membranes (8 ± 0.2 nm; $n = 3$) is not affected by cellular exposure to trypsin (1 mg mL^{-1} for 40 min) prior to detergent solubilization. However, red cell exposure to DTT (2 mM for 30 min at 37 °C) prior to cholate solubilization reduces the Stokes radius of cholic acid/lipid/GLUT1 micelles from 8 to 5.1 ± 0.3 nm ($n = 3$). Cholic acid-solubilized, purified tetrameric and dimeric GLUT1 are characterized by Stokes radii of 7.8 ± 0.2 and 6.0 ± 0.2 nm, respectively (Hebert & Carruthers, 1992).

Effects of Trypsin on Transporter Photolabeling by Cytochalasin B. GLUT1 present in intact and trypsinized red cells was photolabeled using [^{3}H]cytochalasin B, and the labeled species were resolved by SDS−PAGE. Suboptimal conditions of proteolysis were used in order to aid the comparison of ligand binding to intact and 25 kDa GLUT1

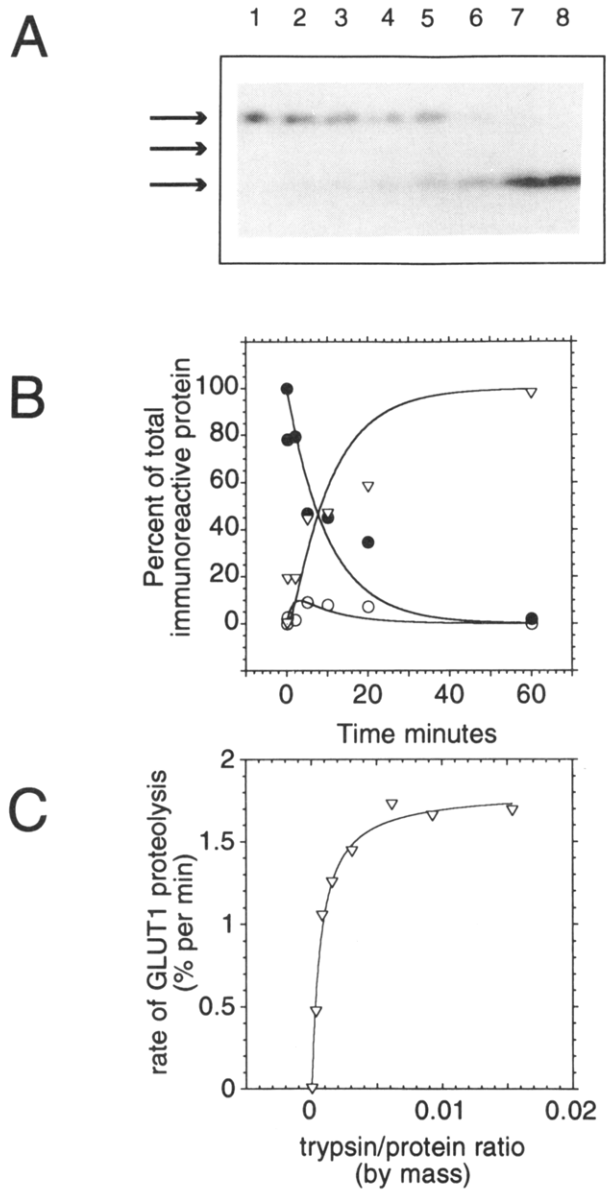

FIGURE 2: Kinetics of GLUT1 digestion by extracellular trypsin. (A) Erythrocytes (5.5×10^9 cells/mL) were digested with 0.3 mg/mL trypsin in HEPES-saline for 0, 2, 5, 10, 20, 30, 45, and 60 min (lanes 1−8 respectively) at 37 °C. Erythrocytes were washed and lysed. Membrane proteins were electrophoresed on 15% polyacrylamide gels and subjected to Western blot analysis using anti-GLUT1 C-terminal antiserum, and immunoreactive proteins were visualized by autoradiography. (B) The intensities of immunoreactive proteins revealed by autoradiography were quantitated by scanning densitometry. Three populations of immunoreactive proteins were quantitated (see arrows in panel A): intact GLUT1 (●), a 38 kDa peptide (○), and a 25 kDa peptide (▽). Curves drawn through the points were computed by fourth-order Runge−Kutta numerical integration by assuming that GLUT1 is initially proteolyzed to release a 38 kDa C-terminal peptide, which is subsequently cleaved to produce a 25 kDa C-terminal peptide. The computed best fit first-order rate constants for assumed first and second cleavage reactions are 0.1 and 0.75 min^{-1} respectively. (C) Concentration dependence of GLUT1 proteolysis by exofacial trypsin. Erythrocytes were digested (as in panel A) for 30 min at varying [trypsin]. Erythrocyte membranes were collected and membrane proteins were processed as in panel A. The extent of GLUT1 proteolysis was quantitated as in panel B. The curve drawn through the points was drawn by eye and has no theoretical significance.

peptides within the same membrane. With trypsinized red cells, most of the incorporated label migrates with low molecular weight species that colocalize with the C-terminal peptide fragment (Figure 4A). This region of the gel contains a greater percentage of photolabel if labeling is performed before the trypsinization of red cells rather than after trypsinization (Figure 4A). The extent of GLUT1 proteolysis is also increased by photolabeling (but not by UV irradiation per se) prior to proteolysis (see inset of Figure 4A). The presence of 50 μM cytochalasin B during red cell exposure to trypsin does not alter the extent of GLUT1 proteolysis (Figure 1B, lanes 2 and 3). It is possible, therefore, that cytochalasin B cross-linking (but not cytochalasin binding per se) promotes exofacial tryptic digestion of GLUT1, but that proteolysis does not prevent ligand binding to the 25 kDa tryptic fragment.

Cytochalasin B binding to the 25 kDa tryptic fragment appears to be increased relative to binding to intact GLUT1. When normalized for the amount of immunodetectable GLUT1 C-terminal peptide (Figure 4A, inset) and corrected for the small amount of endogenous GLUT1 proteolysis detected in control cells (Figure 4A), cytochalasin B photoincorporation into the 25 kDa peptide is 4 ± 1.3-fold greater if labeling is performed after proteolysis rather than before trypsinization ($n = 3$). Label incorporation per unit 25 kDa peptide (fraction of total cpm/fraction of total immunodetectable protein) is 1.75 ± 0.25 (labeled after proteolysis; $n = 4$) versus 0.43 ± 0.23 (labeled before proteolysis; $n = 4$). Label incorporation per unit intact GLUT1 averages 0.39 ± 0.13 ($n = 5$) and is unchanged by exposure to trypsin. This latter finding substantially confirms the central assumption of this analysis (immunostaining is directly proportional to intact GLUT1 and 25 kDa GLUT1 peptide levels) since 25 kDa peptide and intact GLUT1 derived from cells that were photolabeled before proteolysis should be characterized by identical label incorporation efficiencies.

Effects of Trypsin on Equilibrium Cytochalasin B Binding. If increased cytochalasin B photolabeling of the 25 kDa peptide reflects increased binding of ligand (rather than increased photolabeling efficiency), this should be observable at the level of steady state cytochalasin B binding to red cells. We therefore examined the effects of GLUT1 trypsinization on equilibrium cytochalasin B binding. Trypsin-treated RBCs are characterized by a significantly increased capacity to bind cytochalasin B (Table 1). Binding shows simple saturation kinetics in both control and trypsin-treated cells, but maximum cytochalasin B binding (B_{max}) and the apparent dissociation constant $K_{d(app)}$ for cytochalasin B binding are approximately doubled in trypsin-treated cells relative to control cells.

Cytochalasin B binding to intact cells is complicated by nonspecific ligand binding to intracellular hemoglobin (Jung & Rampal, 1977; Helgerson & Carruthers, 1987). We prepared erythrocyte membranes from control and trypsin-treated cells and measured cytochalasin B binding to these nominally hemoglobin-free membranes. B_{max} and $K_{d(app)}$ for binding to control membranes are significantly (almost 2-fold) lower than the corresponding parameters for cytochalasin B binding to membranes prepared from trypsinized red cells (Table 1, Figure 4B). These effects on B_{max} and $K_{d(app)}$ do not reflect trypsin-induced changes in erythrocyte membrane protein content since the red cell membrane protein content (0.6 ± 0.04 pg per erythrocyte) is unchanged following erythrocyte exposure to extracellular trypsin.

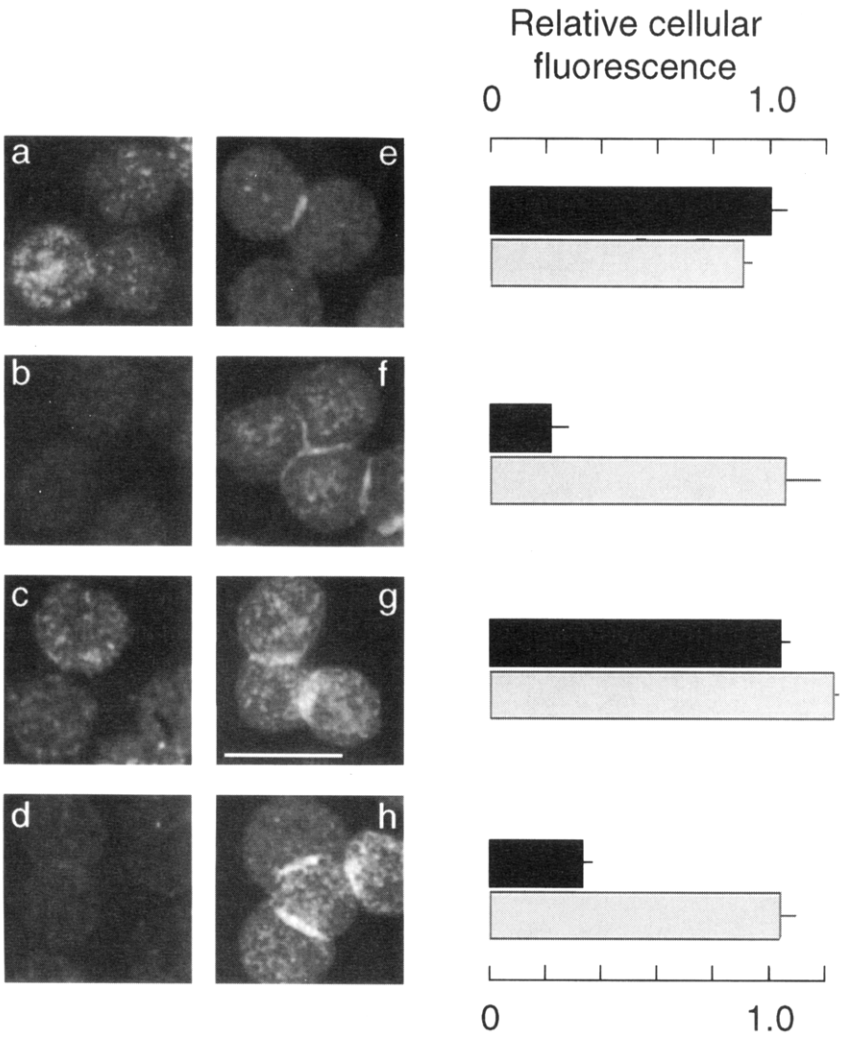

FIGURE 3: Effects of trypsin and reductant on ∂-Ab and C-Ab binding to red cell GLUT1. Antibody binding to permeabilized erythrocytes was quantitated by digital imaging fluorescence microscopy. Cells were preincubated for 30 min at 37 °C with 0.5 mg mL^{-1} trypsin (c, d, g, h) or saline (a, b, e, f) and then attached to coverslips, where they were exposed to saline (a, c, e, g) or 2 mM DTT (b, d, f, h) for 30 min at 37 °C prior to fixation and permeabilization. ∂-Ab binding was measured in a−d. C-Ab binding was measured in e−h. The bar chart to the right of the images quantitates cellular fluorescence (relative to cells in part a) in arbitrary units. Results are shown as mean ± SEM ($n = 5$) for ∂-Ab (black bars) and C-Ab (gray bars). This experiment was repeated three times with quantitatively similar results on each occasion.

Trypsinization of unsealed erythrocyte membranes results in the loss of saturable cytochalasin B binding (Figure 4B, Table 1), while trypsin treatment of GLUT1 proteoliposomes doubles $K_{d(app)}$ for cytochalasin B binding to purified GLUT1 (Table 1).

Because exofacial proteolysis doubles both B_{max} and $K_{d(app)}$ for cytochalasin B binding to intact cells, the ratio B_{max}:$K_{d(app)}$ for cytochalasin B binding to erythrocyte-resident GLUT1 is unchanged by trypsin treatment. Since saturable cytochalasin B binding at low ligand concentrations is described by [cytochalasin B]k, where $k = B_{max}/K_{d(app)}$, this suggests that trypsin treatment should not affect ligand binding at limitingly low ligand concentrations. This was confirmed in experiments where the effects of trypsin treatment on erythrocyte cytochalasin B binding (at low [cytochalasin B]) and 3-*O*-methylglucose uptake were measured. Neither sugar uptake nor ligand binding is affected (Table 2) in spite of extensive GLUT1 proteolysis (Figure 1B, lane 2). In contrast, exposure of control and trypsin-treated cells to 2 mM DTT (a treatment causing transporter dissociation into dimeric GLUT1) inhibits protein-mediated sugar uptake by 2-fold (Table 2).

Effects of Trypsin on the Availability of Exo- and Endofacial Ligand Binding Sites. In the absence of maltose, cytochalasin B binding to control and trypsin-treated red cells is not distinguishable (Figure 4C). However, the manner by which maltose inhibits cytochalasin B binding to GLUT1 is modified significantly following red cell exposure to trypsin. The nature of the antagonistic relationship between exofacial maltose and endofacial cytochalasin B binding sites is revealed (Helgerson & Carruthers, 1987) by expressing the ratio of free [cytochalasin B]:bound [cytochalasin B] as a function of maltose concentration (Figure 4 C). If cytochalasin B and maltose binding sites cannot coexist, the relationship is linear with positive slope. If cytochalasin B and maltose binding sites coexist but interact with negative cooperativity, the relationship is positively curvilinear. Figure 4C shows that, prior to exofacial proteolysis, exofacial maltose and endofacial cytochalasin B binding sites interact with negative cooperativity. Following proteolysis, however, cytochalasin B and maltose binding sites are mutually exclusive. The effect of trypsin on maltose inhibition of cytochalasin B binding to red cell GLUT1 is not further

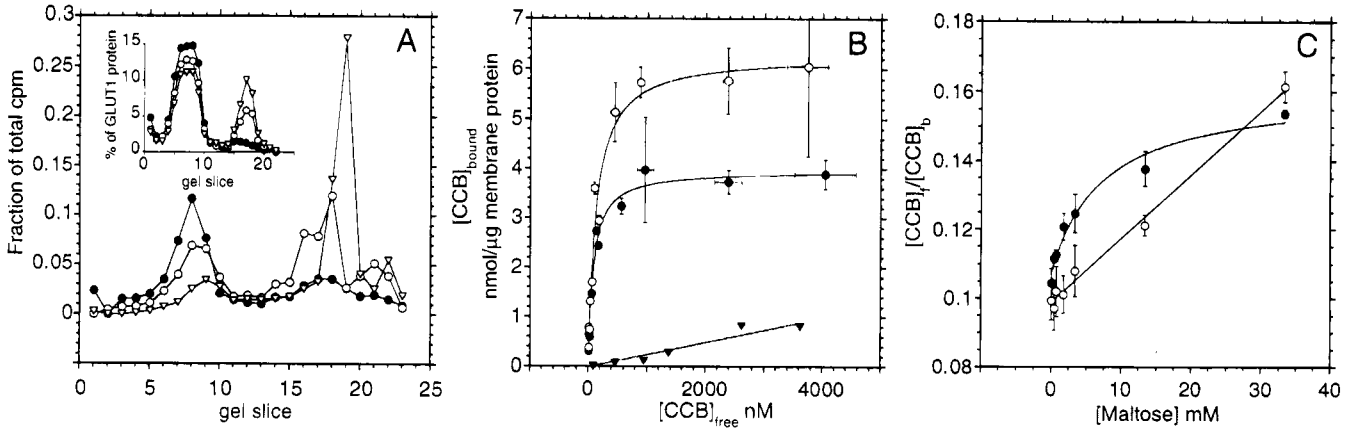

FIGURE 4: Effect of trypsin on GLUT1-mediated ligand binding. (A) Erythrocytes were photolabeled using [^{3}H]cytochalasin B either before (▽) or after (○) exposure to 50 μg mL^{-1} trypsin for 30 min. at 37 °C. Control (trypsin-free) cells are also shown (●). Erythrocytes were washed and lysed, and membrane proteins were electrophoresed on 10% gels. Gels were stained with Coomassie Brilliant Blue and then destained, and gel lanes were sliced into 2 mm aliquots. Each gel slice was digested with 10% H_2O_2 at 56 °C overnight and then analyzed by liquid scintillation counting. The inset shows the densitometric quantitation of an autoradiogram of a parallel Western blot analysis of these membranes using anti-GLUT1 C-terminal antiserum. DPM of [^{3}H]cytochalasin B incorporated per lane are as follows: control, 5453; labeled before trypsin, 6439; labeled after trypsin, 8683. (B) Effect of trypsin on cytochalasin B binding to membranes isolated from intact cells (●), intact cells exposed to 100 μg mL^{-1} trypsin for 30 min at 37 °C (○), or unsealed erythrocyte membranes exposed to 100 μg mL^{-1} trypsin for 30 min at 37 °C (▼). Curves drawn through intact cell data (●, ○) were computed by nonlinear regression assuming simple saturable binding. Computed binding constants are as follows: control (●), $K_{d(app)} = 83 \pm 12$ nM, $B_{max} = 3.9$ pmol/μg membrane protein; trypsin (○), $K_{d(app)} = 126 \pm 21$ nM, $B_{max} = 6.3 \pm 0.3$ pmol/μg membrane protein. Each data point represents the mean ± SEM of at least four separate measurements made in duplicate. The membrane protein content of intact cells (0.6 ± 0.04 pg per cell) is not significantly altered by trypsin exposure. The protein content of unsealed erythrocyte membranes is depleted by trypsin exposure. Here (▼), binding measurements were made using an equivalent number of cell unit membranes. (C) Effect of trypsin on maltose inhibition of cytochalasin B binding to erythrocytes. Intact cells (●) and trypsin treated (1 mg mL^{-1} for 30 min at 37 °C) cells (○) were exposed to saline containing 100 nM cytochalasin B and varying (0−33 mM) maltose concentrations osmotically balanced using sucrose. Cytochalasin B binding was measured at 4 °C. Each data point represents the mean ± SEM of nine separate measurements. Curves drawn through the points were computed by nonlinear regression assuming that binding is described by the relationship (Helgerson & Carruthers, 1987), $[CCB_f]/[CCB_b] = [CCB_f]/[X_t] + (K_i/[X_t])\{(K_o + [\text{maltolse}])/(K_o + [\text{maltose}]/\alpha)\}$, where CCB_f and CCB_b are free and bound cytochalasin B, respectively, X_t is glucose transporter, K_i and K_o are the dissociation constants for cytochalasin B and maltose, respectively, binding to X_t, and α is the negative cooperativity factor. For control cells, the computed best fit ($R^2 = 0.972$) is obtained using the following constants: $[X_t] = 1.8$ μM, $K_i = 0.1$ μM, $K_o = 3.6$ mM, and $\alpha = 2.0$. For trypsin-treated cells, the computed best fit ($R^2 = 0.992$) is obtained using the following constants: $[X_t] = 4.3$ μM, $K_i = 0.33$ μM, $K_o = 40.8$ mM, and $\alpha > 2 \times 10^{14}$.

Table 2: Effect of Trypsin on Sugar Transport and Ligand Binding at Limiting Substrate Levels

	control[a]		trypsin	
	saline	+DTT	saline	+DTT
3OMG uptake[b]				
control	152.1 ± 0.4	75.6 ± 1.2	132.9 ± 2.3	78.6 ± 0.5
plus CCB[c]	5.8 ± 0.7	4.4 ± 0.5	5.4 ± 0.3	4.7 ± 0.2
CCB binding[d]				
control	10.01 ± 0.36	7.43 ± 0.68	9.51 ± 0.21	6.97 ± 0.33
plus phloretin[e]	1.9 ± 0.2	1.8 ± 0.2	1.7 ± 0.3	1.8 ± 0.1

[a] All experiments are paired experiments (control versus 1 h of trypsin treatment at 1 mg of trypsin per 10^{10} cells ± 2 mM dithiothreitol, pH 7.4). The number of paired determinations made in triplicate is three or more. [b] 3-*O*-Methylglucose uptake (at 100 μM) was measured at 4 °C and is expressed as micromoles of sugar transported per liter cell water per minute. [c] Uptake was measured in the presence of the sugar transport inhibitor cytochalasin B (50 μM; $K_{i(app)}$ for transport inhibition = 350 nM). [d] Cytochalasin B binding is expressed as the ratio bound [cytochalasin B]:free [cytochalasin B]. The concentration of free cytochalasin B at equilibrium was approximately 30 nM. [e] Cytochalasin B binding was also measured in the presence of 100 μM phloretin, a cytochalasin B binding antagonist.

modified by subsequent cellular exposure to 2 mM DTT (37 °C for 30 min; $n = 3$).

Effects of Trypsin on the 3-O-Methylglucose Transport. Neither V_{max} nor $K_{m(app)}$ for net 3-*O*-methylglucose uptake by erythrocytes is affected significantly by trypsin treatment (Table 3). Net 3-*O*-methylglucose uptake by both control and trypsinized erythrocytes is inhibited significantly by 2 mM dithiothreitol (Table 2). Cytochalasin B inhibition of net 3-*O*-methylglucose uptake is unaffected in trypsin-treated cells (Table 3). Prior trypsin treatment is without effect on subsequent tracer (60 μM) 3-*O*-methylglucose efflux from erythrocytes at ice temperature (rate constant for exit from control and trypsin-treated cells = 0.18 ± 0.03 and 0.20 ± 0.02 min^{-1}, respectively; $n = 3$). Basal cell membrane permeability is unchanged by trypsin treatment, as 3-*O*-methylglucose uptake in the presence of 10 μM cytochalasin B is unaffected by prior cell exposure to trypsin (Table 3). It is unlikely, therefore, that trypsin penetrates cells to alter GLUT1 structure−function when the monosaccharide, 3-*O*-methylglucose, is excluded by the membrane bilayer.

$K_{m(app)}$ for protein-mediated D-glucose transport by reconstituted GLUT1 proteoliposomes is reduced 2-fold by exofacial trypsin treatment, but V_{max} for uptake is reduced by only 20% (Figure 5 and Table 2). The fall in reconstituted transport activity (20%) upon trypsin treatment of proteoliposomes is close to the expected decline of 37%. Under

Table 3: Effect of Extracellular Trypsin on GLUT1-Mediated Sugar Transport

		control[a]	trypsin
proteoliposome D-glucose uptake[b]	V (mM/min)[c]	58.8 ± 2.3	47.2* ± 1.6
	K_m (mM)[c]	8.6 ± 0.5	4.6* ±0.2
red cell 3OMG uptake[d]	V_{max} (μM/min)	241 ± 17	212 ± 10
	K_m (mM)	0.7 ± 0.1	1.2 ± 0.1
CCB inhibition of red cell 3OMG uptake[e]	I_m (%)	86 ± 11	87 ± 16
	$K_{i(app)}$ (nM)	419 ±113	359 ± 101

[a] All experiments are paired experiments (control versus trypsin treatment). The number of paired determinations made in duplicate is three or greater. *Indicates that the result is significantly different from the control measurement ($p < 0.05$, 1 tailed t-test). [b] D-Glucose (100 mM) uptake by proteoliposomes was measured at 24 °C. Proteoliposomes (20 μg of GLUT1) were exposed to trypsin-free saline or to saline containing 5 μg of trypsin for 30 min. [c] V is the computed maximum rate of 3-*O*-methylglucose uptake, while K_m is that concentration of intraliposomal 3-*O*-methylglucose that produces 0.5 V. [d] 3-O-Methylglucose uptake by erythrocytes was measured at 0−4 °C. Cells (10^9) were exposed to saline or to saline containing 0.3 mg mL^{-1} trypsin for 30 min at 37 °C. [e] Cytochalasin B inhibition of red cell 3-*O*-methylglucose uptake from medium containing 2 mM 3-*O*-methylglucose was analyzed by nonlinear regression assuming simple saturation kinetics. I_m is the maximum inhibition (%) produced by cytochalasin B, while $K_{i(app)}$ is that concentration of cytochalasin B that produces 0.5 I_m. Cells (10^9) were exposed to saline or to saline containing 0.3 mg mL^{-1} trypsin for 30 min at 37 °C.

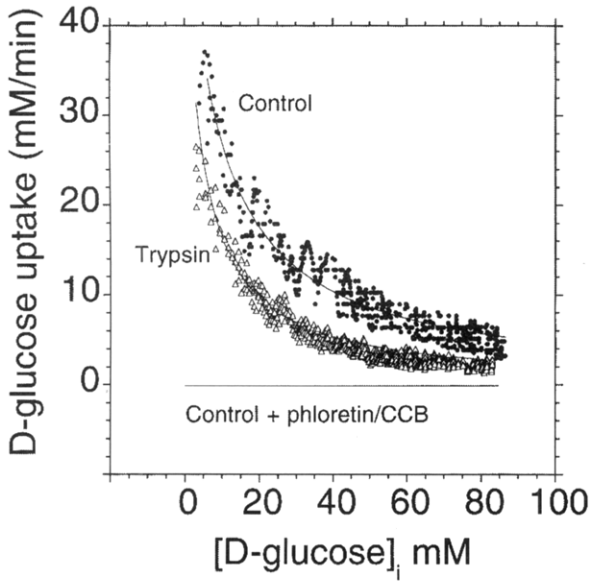

FIGURE 5: Effect of trypsin on GLUT1-mediated D-glucose uptake by reconstituted proteoliposomes. Key: ●, control proteoliposomes; △, trypsin-treated proteoliposomes (see Figure 1C for details); — (straight line indicating no measurable transport), uptake by proteoliposomes exposed to 100 μM phloretin plus 50 μM cytochalasin B or by proteoliposomes formed from GLUT1 that was trypsin-treated prior to reconstitution by cholate dialysis. The rate of sugar uptake at each [D-glucose]$_i$ was computed as the first-order derivative of the time course of D-glucose uptake. The curves drawn through the points were computed by nonlinear regression assuming Michaelis−Menten kinetics and have the following parameters: control, $V = 56 \pm 1.9$, $K_{m(app)} = 9.2 \pm 0.5$; trypsin, $V = 47.2 \pm 1.6$, $K_{m(app)} = 4.6 \pm 0.2$. V has units of millimolar per minute and corresponds to the rate of D-glucose uptake when intravesicular D-glucose is absent. $K_{m(app)}$ has units of millimolar and corresponds to that concentration of intravesicular D-glucose that reduces sugar uptake to 0.5 V. These data summarize five separate experiments.

the conditions of these experiments, trypsin treatment of GLUT1 proteoliposomes results in the loss of detectable protein (Figure 1C, lane 2), as judged by Coomassie staining of control and trypsin-treated proteoliposomes resolved by SDS−PAGE. Protein-mediated sugar transport activity is undetectable in proteoliposomes containing GLUT1 exposed to trypsin prior to reconstitution (Figure 5).

DISCUSSION

This study demonstrates that the backbone of the erythrocyte glucose transport protein can be broken at two extracellular sites without ablating protein-mediated sugar transport. In the process, however, the glucose transporter is converted from a multisite transporter (Carruthers & Helgerson, 1991) to a simple carrier (Widdas, 1952). Previous studies have shown that trypsin cleaves GLUT1 at multiple intracellular sites and that the resulting transporter is nonfunctional (Baldwin et al., 1980; Cairns et al., 1987; Carruthers & Melchior, 1983; Holman & Rees, 1987; Masaik & LeFevre, 1977; Mueckler et al., 1985). These studies also concluded that GLUT1 was not cleaved at extracellular sites since transport function was unchanged by exofacial trypsin. We show here that GLUT1 is indeed cleaved at the exofacial surface, not once but twice. Proteolysis abolishes cooperative interactions between substrate binding sites, but leaves transport activity and transporter oligomeric structure unchanged.

The time course of extracellular tryptic digestion of GLUT1 suggests that a rapid initial cleavage is followed by a second cleavage. The first cut releases a low-abundance, C-terminal peptide of estimated M_r 38 000. Within 30 min, this intermediate disappears, yielding a 25 kDa peptide. It is possible that the initial cleavage is necessary to provide access to the second cleavage site, resulting in the appearance of the 25 kDa peptide. If we assume that this model is correct, our calculations suggest rate constants for the first and second cleavage reactions of 0.1 and 0.75 min^{-1}, respectively (see Figure 2B). An alternative explanation is that the red cell exposes two populations of GLUT1. The smaller population (10% of total GLUT1) is hydrolyzed slowly ($k = 0.1$ min^{-1}) to release a 38 kDa fragment, which is then rapidly degraded ($k = 0.5$ min^{-1}). The larger population (>90% of total GLUT1) is cleaved slowly (rate constant = 0.1 min^{-1}) to release the 25 kDa fragment. The available data do not allow us to distinguish between these possibilities.

The 25 kDa GLUT1 tryptic fragment contains an intact C-terminus since this peptide is detected on Western blot analysis using anti-GLUT1 C-terminal peptide antiserum. The electrophoretic mobilities of intact GLUT1 and both immunodetectable, C-terminal GLUT1 tryptic fragments on 15% acrylamide gels are consistent with molecular masses of 64.2 ± 1.3, 38.3 ± 0.9, and 25.2 ± 1.2 kDa respectively ($n = 7$). If we assume that this analysis is correct, potential tryptic cleavage sites are arginine$_{153}$ (M_r = 37 700) and arginine$_{264}$ (M_r = 25 100). However, hydropathy and glycosylation scanning mutagenesis analyses (Mueckler et al.,

1985; Hresko et al., 1994a) suggest that these sites lie inside the cell, and antipeptide antibody binding studies indicate that a GLUT1 region immediately N-terminal to arginine$_{264}$ (residues 218−232) is cytoplasmic (Andersson & Lundahl, 1988). GLUT1 and other membrane proteins that bind sodium dodecyl sulfate more avidly than do more hydrophilic proteins can show anomalous electrophoretic behavior upon SDS−PAGE. For example, intact GLUT1 and the smaller C-terminal GLUT1 tryptic fragment are resolved as 56.4 ± 0.7 and 17.5 ± 1.8 kDa peptides, respectively, in 10% acrylamide gels (n = 4; Figure 1B). Similarly, RhD (band 7 protein with deduced molecular mass 45.2 kDa) is resolved as a 33 kDa peptide upon electrophoresis in 10% acrylamide gels (Zottola et al., 1995). It is not possible, therefore, to make precise assignments of sites of GLUT1 proteolysis on the basis of an analysis of peptide maps alone. The N-terminal sequence of the 25 kDa fragment is required. If we assume that the proposed membrane topography of GLUT1 is correct, hydrolysis at exofacial residues lysine$_{183}$ and lysine$_{300}$ would produce peptides of M_r 34 400 and 20 800, respectively, with theoretical relative mobilities of 0.6:1 [compare with experimental value of (0.65 ± 0.05): 1].

GLUT1-mediated sugar transport in reconstituted GLUT1 proteoliposomes is resistant to trypsin inhibition, while reconstitution of trypsin-treated GLUT1 by detergent dialysis fails to reconstitute glucose transport. This suggests that GLUT1 function and essential noncovalent GLUT1 structure are maintained when the proteolyzed transporter is embedded in the membrane bilayer, but are lost during the reconstitution process.

Red cell resident GLUT1 oligomeric structure was examined by two methods: size-exclusion chromatography and analysis of ∂-Ab binding. The former method provides information on the hydrodynamic radius of particles released from the red cell membrane upon detergent solubilization (Hebert & Carruthers, 1991). The latter method provides information on the surface accessibility of tetrameric GLUT1-specific epitopes (Hebert & Carruthers, 1992).

Size-exclusion analysis of cholate-solubilized red cell membranes indicates that prior cell exposure to trypsin does not change the Stokes radius (8 nm) of lipid/detergent micelles containing GLUT1 and GLUT1−carboxyl-terminal peptides. While these particles may contain non-GLUT1 protein species, they also coelute with authentic tetrameric GLUT1 (Stokes radius = 8 nm). ∂-Ab-reactive epitopes are lost in reductant-treated but not in trypsin-treated cells. Our analyses demonstrate that ∂-Ab reacts with membrane-resident, tetrameric GLUT1 and SDS-denatured, reduced GLUT1, but not with reduced, membrane-resident (dimeric) GLUT1 [see present work and Hebert and Carruthers, (1992)]. The results of our current analyses, therefore, support the conclusion that exofacial, tryptic digestion of GLUT1 does not cause dissociation of the multisubunit transporter complex. Exposure to extracellular reductant, however, promotes a significant GLUT1 conformational change, resulting in transporter dissociation and occlusion of cell surface (∂-Ab-reactive) epitope(s). While it is formally possible that ∂-Ab-reactive epitopes could be lost under circumstances where GLUT1 tetrameric structure is maintained, or that ∂-Ab binding could be retained under conditions where GLUT1 dissociates into dimers, neither of these possibilities has been observed experimentally [see present work and Hebert and Carruthers (1992)].

Steady state cytochalasin B binding to glucose transporter present in trypsin-treated cells is almost twice that measured in untreated cells. This increased ligand binding capacity is also seen in erythrocyte ghosts prepared from trypsin-treated red cells. The increase in red cell cytochalasin B binding promoted by trypsin is not explained by a trivial loss of membrane protein, because exposure to exofacial trypsin does not alter erythrocyte membrane protein content significantly. Furthermore, our analyses suggest that the 25 kDa GLUT1 C-terminal peptide is photolabeled by cytochalasin B 4 ± 1.3-fold more efficiently than is intact GLUT1. This analysis assumes that intact GLUT1 and the 25 kDa peptide share equal blotting affinity for C-Ab. This increased binding quantitatively accounts for the increase in steady state ligand binding capacity of red cell membranes and confirms previous demonstrations of suppressed, erythrocyte-resident GLUT1 cytochalasin B binding potential (Hebert & Carruthers, 1991, 1992).

The photolabeled, intact transporter is proteolyzed more efficiently than nonlabeled GLUT1 or the cytochalasin B−GLUT1 equilibrium complex. Because equilibrium cytochalasin B binding does not enhance GLUT1 exofacial proteolysis, this suggests that the covalently (cytochalasin B) liganded transporter is conformationally distinct from its noncovalently (cytochalasin B) liganded and unliganded counterparts. These conclusions are consistent with those of other studies (Holman & Rees, 1987; Karim et al., 1987). While the cytochalasin B binding capacity of membranes isolated from trypsin-treated red cells is doubled, the affinity of the membranes for cytochalasin B is halved ($K_{d(app)}$ is approximately doubled). This result [which is consistent with unchanged cytochalasin B binding at low ligand concentrations; see present work and Baldwin et al., (1980)] is equivalent to the loss of one van der Waals bond between cytochalasin B and its binding site. In contrast, $K_{d(app)}$ for D-glucose binding to the sugar influx site and $K_{m(app)}$ for 3-*O*-methylglucose uptake are unchanged, while $K_{d(app)}$ for D-glucose binding to the sugar efflux site and $K_{m(app)}$ for D-glucose exit from proteoliposomes are reduced 2−4-fold by trypsin treatment. Although interpretation of the latter effect is complicated by the random orientation of GLUT1 in reconstituted proteoliposomes, the evidence suggests that GLUT1 proteolysis exerts contrasting actions on the binding of two distinct ligands at the sugar efflux site.

The transported substrates (D-glucose and 3-*O*-methylglucose) bind with increased affinity to proteolyzed GLUT1, while the nontransported, inhibitory ligand cytochalasin B binds with reduced affinity. These observations are consistent with the action of intra- plus extracellular trypsin on ligand binding to purified GLUT1 (Cairns et al., 1984) and support the view that cytochalasin B and intracellular sugar binding to the transporter, although mutually exclusive, is not mediated by identical chemistries (Cairns et al., 1987; Carruthers & Helgerson, 1991; Holman & Rees, 1987). Transported and nontransported (but reactive) ligands have previously been shown to promote different actions at GLUT1 substrate binding sites. Binding of nontransported species imparts negative cooperativity between import and export, sites while binding of transported species does not (Helgerson & Carruthers, 1987).

How is it possible that sugar transport in control and trypsinized cells is indistinguishable, while cytochalasin B binding to trypsinized cells is doubled? The simplest explanation is that the increase in cytochalasin B binding is not associated with the glucose transporter. Trypsinization reveals cryptic, non-GLUT1 sites with reduced affinity for ligand (relative to GLUT1). This seems unlikely since extracellular maltose inhibits the increase in binding produced by trypsin. In addition, photoaffinity labeling experiments indicate that the increased binding is associated with the 25 kDa GLUT1 carboxyl-terminal peptide.

An alternative explanation is that cooperative interactions between subunits of the oligomeric transporter complex are relaxed upon exofacial proteolysis of GLUT1. The erythrocyte sugar transporter is a GLUT1 tetramer (Hebert & Carruthers, 1991, 1992). Each subunit (GLUT1 protein) contributes a single sugar transport site to the transporter complex and at any time can expose either a sugar import or a sugar export site (but not both) to available substrate. It has been proposed that cooperative interactions between subunits produce an antiparallel arrangement of subunit transport sites (two uptake and two efflux sites) at all times (Hebert & Carruthers, 1992). Thus, if one subunit exposes a sugar export site, the adjacent subunit must expose a sugar import site and vice versa. Since cytochalasin B binds at or very close to the sugar efflux site and each subunit can expose only a sugar uptake or a sugar efflux site (but not both) at any instant, each GLUT1 tetramer can bind only two molecules of cytochalasin B. Tetrameric GLUT1 dissociates into GLUT1 dimers when exposed to reductant [see present work here and Hebert and Carruthers (1991, 1992)]. Cooperative interactions between subunits are relaxed in dimeric GLUT1, and the antiparallel arrangement of binding sites is lost. The cytochalasin B binding capacity of dimeric GLUT1 thus is twice that of the native, tetrameric transporter. The proteolyzed glucose transport may, therefore, functionally resemble the reduced, dimeric transporter.

This hypothesis does not require that relaxation of catalytic cooperativity between subunits is accompanied by dissociation of tetrameric GLUT1 into GLUT1 dimers (although the reverse would be required). However, the theory does predict that loss of cooperativity between subunits inhibits GLUT1-mediated sugar transport and abolishes negative cooperativity between cytochalasin B (sugar efflux) and exofacial maltose (sugar influx) binding sites (Hebert & Carruthers, 1992). Our experiments show that proteolyzed GLUT1 retains structural features unique to tetrameric GLUT1, suggesting that the transporter does not dissociate into GLUT1 dimers. Our experiments also show that V_{max} for 3-*O*-methylglucose uptake is unaffected by trypsin treatment of red cells. However, trypsin releases exofacial maltose and endofacial cytochalasin B binding sites from obligate, negative, cooperative interactions and renders these sites mutually exclusive. This is a methodologically independent replication of the action of reductant on ligand binding to the glucose transporter (Hebert & Carruthers, 1991, 1992). In this instance, however, cooperativity between transporter subunits is lost under circumstances where structurally cohesive interactions between subunits appear to be maintained.

Red cell exposure to reductant mimics the ability of trypsin to inhibit cooperative interactions between substrate binding sites (Zottola et al., 1995), but also causes sugar import inhibition and subunit dissociation (as judged by the loss of tetramer-specific GLUT1 epitopes and the reduced Stoke's radius of the detergent-solubilized transporter). This suggests that maintenance of tetrameric structure, but not cooperativity between subunit binding sites, is required for efficient catalytic turnover. Provided that GLUT1 proteolysis does not introduce as yet uncharacterized compensatory changes in subunit catalytic turnover, the hypothesized antiparallel arrangement of substrate binding sites cannot directly contribute to catalytic efficiency as was originally proposed (Hebert & Carruthers, 1992).

In conclusion, our studies demonstrate that GLUT1 is vulnerable to proteolysis by trypsin at at least one extracellular site. This disruption of glucose transporter covalent structure is not accompanied by detectable changes in transporter oligomeric structure, nor does it abrogate sugar transport function. Exofacial proteolysis does, however, destroy cooperative interactions between subunits, allowing each subunit to behave as a simple carrier. This relaxation of obligate, antiparallel, catalytic conformations in adjacent subunits renders sugar import and sugar export sites mutually exclusive, reveals the full cytochalasin B binding potential of GLUT1 (1 mol of cytochalasin B per mole of GLUT1), and indicates that cooperative substrate binding is not necessary for high catalytic turnover. At this time, it is uncertain whether the loss of catalytic cooperativity results from direct proteolysis of a critical interfacial domain between subunits or from indirect proteolysis-induced disorder in crucial interfacial domains distal to the site(s) of covalent rupture.

REFERENCES

Andersson, L., & Lundahl, P. (1988) *J. Biol. Chem. 263*, 11414−11420.

Appleman, J. R., & Lienhard, G. E. (1989) *Biochemistry 28*, 8221−9227.

Baldwin, J. M., Lienhard, G. E., & Baldwin, S. A. (1980) *Biochim. Biophys. Acta 599*, 699−714.

Cairns, M. T., Elliot, D. A., Scudder, P. R., & Baldwin, S. A. (1984) *Biochem. J. 221*, 179−188.

Cairns, M. T., Alvarez, J., Panico, M., Gibbs, A. F., Morris, H. R., Chapman, D., & Baldwin, S. A. (1987) *Biochim. Biophys. Acta 905*, 295−310.

Carruthers, A. (1986a) *Biochemistry 25*, 3592−3602.

Carruthers, A. (1986b) *J. Biol. Chem. 261*, 11028−11037.

Carruthers, A. (1990) *Physiol. Rev. 70*, 1135−1176.

Carruthers, A. (1991) *Biochemistry 30*, 3898−3906.

Carruthers, A., & Melchior, D. L. (1983) *Biochim. Biophys. Acta 728*, 254−266.

Carruthers, A., & Melchior, D. L. (1984a) *Biochemistry 23*, 6901−6911.

Carruthers, A., & Melchior, D. L. (1984b) *Biochemistry 23*, 2712−2718.

Carruthers, A., & Helgerson, A. L. (1991) *Biochemistry 30*, 3907−3915.

Chin, J. J., Jhun, B. H., & Jung, C. Y. (1992) *Biochemistry 31*, 1945−1951.

Czech, M. P., & Buxton, J. M. (1993) *J. Biol. Chem. 268*, 9187−9190.

De Vivo, D. C., Trifiletti, R. R., Jacobson, R. I., Ronen, G. M., Behmand, R. A., & Harik, S. I. (1991) *New Engl. J. Med. 325*, 703−709.

Diamond, D., & Carruthers, A. (1993) *J. Biol. Chem. 268*, 6437−6444.

Fukumoto, H., Kayano, T., Buse, J. B., Edwards, Y., Pilch, P. F., Bell, G. I., & Seino, S. (1989) *J. Biol. Chem. 264*, 7776−7779.

Gould, G. W., & Holman, G. D. (1993) *Biochem. J. 295*, 329−341.

Harik, S. I. (1992) *Can. J. Physiol. Pharmacol. 70*, S113−S117.

Harrison, S. A., Buxton, J. M., Helgerson, A. L., MacDonald, R. G., Chlapowski, F. J., Carruthers, A., & Czech, M. P. (1990) *J. Biol. Chem. 265*, 5793−5801.
Harrison, S. A., Buxton, J. M., & Czech, M. P. (1991) *Proc. Natl. Acad. Sci. USA 88*, 7839−7843.
Hebert, D. N., & Carruthers, A. (1991) *Biochemistry 30*, 4654−4658.
Hebert, D. N., & Carruthers, A. (1992) *J. Biol. Chem. 267*, 23829−23838.
Helgerson, A. L., & Carruthers, A. (1987) *J. Biol. Chem. 262*, 5464−5475.
Helgerson, A. L., & Carruthers, A. (1989) *Biochemistry 28*, 4580−4594.
Helgerson, A. L., Hebert, D. N., Naderi, S., & Carruthers, A. (1989) *Biochemistry 28*, 6410−6417.
Holman, G. D., & Rees, W. D. (1987) *Biochim. Biophys. Acta. 897*, 395−405.
Hresko, R. C., Kruse, M., Strube, M., & Mueckler, M. (1994) *J. Biol. Chem. 269*, 20482−20488.
Janoshazi, A., & Solomon, A. K. (1993) *J. Membr. Biol. 132*, 167−178.
Jung, C. Y., & Rampal, A. L. (1977) *J. Biol. Chem. 252*, 5456−5463.
Jung, C. Y., Hsu, T. L., Cha, J. S., & Haas, M. N. (1980) *J. Biol. Chem. 225*, 361−364.
Karim, A. R., Rees, W. D., & Holman, G. D. (1987) *Biochim. Biophys. Acta 902*, 402−405.
Laemmli, U. K. (1970) *Nature 270*, 680−685.
Lowe, A. G., & Walmsley, A. R. (1986) *Biochim. Biophys. Acta 857*, 146−154.
Maher, F., Vannucci, S. J., & Simpson, I. A. (1993) *J. Cereb. Blood Flow Metab. 13*, 342−345.
Masaik, S. J., & LeFevre, P. G. (1977) *Biochim. Biophys. Acta 465*, 371−377.
Mueckler, M. (1993) *J. Diabetes Complications 7*, 130−141.
Mueckler, M., Caruso, C., Baldwin, S. A., Panico, M., Blench, I., Morris, H. R., Allard, W. J., Lienhard, G. E., & Lodish, H. F. (1985) *Science 229*, 941−945.
Naftalin, R. J. (1988) *Biochim. Biophys. Acta 946*, 431−438.
Naftalin, R. J., & Holman, G. G. (1977) in *Membrane Transport in Red Cells* (Ellory, J. C., & Lew, V. L., Eds.) pp 257-300, Academic Press, New York.
Naftalin, R. J., & Rist, R. J. (1994) *Biochim. Biophys. Acta 1191*, 65−78.
Pessino, A., Hebert, D. N., Woon, C. W., Harrison, S. A., Clancy, B. M., Buxton, J. M., Carruthers, A., & Czech, M. P. (1991) *J. Biol. Chem. 266*, 20213−20217.
Sogin, D. C., & Hinkle, P. C. (1980) *Proc. Natl. Acad. Sci. U.S.A. 77*, 5725−5729.
Stein, W. D. (1986) in *Transport Across Cell Membranes*, pp 231−305, Academic Press, New York.
Takata, K., Kasahara, T., Kasahara, M., Ezaki, O., & Hirano, H. (1992a) *Invest. Opth. Vis. Sci. 33*, 377−383.
Takata, K., Kasahara, T., Kasahara, M., Ezaki, O., & Hirano, H. (1992b) *Cell Tissue Res. 267*, 407−412.
Waddell, I. D., & Burchell, A. (1993) *Eur. J. Pediatr. 152*, S14−S17.
Waddell, I. D., Zomerschoe, A. G., Voice, M. W., & Burchell, A. (1992) *Biochem. J. 286*, 173−177.
Widdas, W. F. (1952) *J. Physiol. (London) 118*, 23−39.
Zeidel, M. L., Albalak, A., Grossman, E., & Carruthers, A. (1992) *Biochemistry 31*, 589−596.
Zottola, R. J., Cloherty, E. K., Coderre, P. E., Hansen, A., Hebert, D. N., & Carruthers, A. (1995) *Biochemistry* (in press).

BI950344F